2017 International Nuclear Atlantic Conference - INAC 2017
Belo Horizonte, MG, Brazil, October 22-27, 2017
ASSOCIAÇÃO BRASILEIRA DE ENERGIA NUCLEAR – ABEN

Agência Brasileira do ISBN
ISBN 978-85-99141-07-6
9 788599 141076

Study on welding thermal cycle and residual stress of UNS S32304 duplex steel selected as external shield for a transport packaging of Mo-99

Evandro G. Betini[1]; Maurilio P. Gomes[1]; Mariana X. Milagre[1]; Caruline S. C. Machado[1]; Luis A. M. Reis[1]; Cristiano S. Mucsi [1]; Marcos T. D. Orlando[2]; Temístocles S. Luz[2]; Jesualdo L. Rossi[1]

[1] Instituto de Pesquisas Energéticas e Nucleares (IPEN / CNEN - SP)
Av. Professor Lineu Prestes 2242
05508-000 São Paulo, SP
egbetini@ipen.br

[2] Departamento de Física –DFIS- Centro de Ciências Exatas -CCE
Universidade Federal do Espirito Santo - UFES
Av. Fernando Ferrari, 514
29075-910 -Vitória , ES – Brazil
mtdorlando@gmail.com

ABSTRACT

Thin plates of duplex stainless steel UNS S32304 were welded using the pulsed gas tungsten arc GTAW process (butt joint) without filler addition. The used shielding gas was pure argon and 98% argon plus 2% of nitrogen. The thermal cycles were acquired during welding, in regions near the melting pool. This alloy is candidate for the external clad of a cask for the transport of high activity radiopharmaceuticals substances. For the residual stress measurements in austenite phase an X-ray diffractometer was used in a Bragg-Brentano geometry with CuKα radiation (λ= 0.154 nm) and for ferrite phase was used a pseudo-parallel geometry with CrKα radiation (λ= 0.2291 nm). The results of residual stress using $\sin^2\psi$ methodology shown that the influence of the high welding temperature leads to compressive stresses in for both phase of the duplex steels mainly in heat-affected zone. It was observed a high temperature peak and an increase of the mean residual stress after addition of nitrogen to the argon shielding gas.

1. INTRODUCTION

The packaging or cask for transport of substances of high radioactivity sources requires high thermo-mechanical protection; mainly the tungsten/tungsten alloys or depleted uranium shielded devices are used for the transport of the Mo-99 with activity above 0.6 TBq (16.2Ci) [1,2]. The increased reliability of the welding process on duplex stainless steels (DSS's) for applications in the nuclear industry endorse the choice this material as external shield for Type B packages [3,4].

The Brazilian National Nuclear Energy Commission - CNEN standard [5] defines the key safety parameters for the design, project and validation tests of the transport devices for radioactive materials. The main rules established for external recipient of Type B packages are the thermal and mechanical tests. The first one consists in fully enclose the sample in a fire presenting average flame temperature of 800 °C for 30 minutes without loss or dispersal of the radioactive content. For mechanical properties is request a fracture strain of 345 MPa and at 189 GPa, for Young's modulus (minimum values accepted). As discussed for the thermal and impact protection, it is interesting that the material used in the external recipient part presents a low density around 8100 $kg.m^{-3}$. In order to deal with this, in study about

selection of materials for a new Type B package produced by Hara et al [1] define that the material selected for external recipient were in the family of steels and nickel (Ni) alloys. However, the stainless steels present a significantly reduced price when compared to Ni alloys, showing advantage in their choice [1].

The modern duplex stainless steels - DSS's have basically ferritic-austenitic microstructure (around 50 - 50 %) that combines excellent properties when high corrosion resistance and superior mechanical properties are required. Associated to a competitive cost, the DSS also have satisfactory weldability [3].

Despite the great advantages there are also some limitations generated during exposure the materials to high welding temperatures. For the welding cycle, thermal strains are induced in all regions near to the weld [6]. Accompanied of the thermal strains a plastic upsetting is produced. The thermal stresses resulting from these strains combine and react to produce internal forces that cause residual stress [7]. In previous work, Machado et al [8] studied the effect of the shielding gas composition on the residual stress distribution in austenite phase of the duplex stainless steel welds. Concerning the radiation influences, Cárcel-Carrasco et al [9] investigated the effect of low-level ionizing X-rays on the micro structural characteristics, resistance, and corrosion resistance of TIG-welded joints of AISI 304 steels using AISI 316L filler rods. It was observed that welds subjected to doses of 1000 Gy of ionizing radiation have an influence on the resistance and corrosion characteristics, and this is especially true for welds made in a conventional atmosphere. In this way, careful about these failures are even greater when dealing with the transportation of radioactive products.

For each type of stress state it is associated one or a combination of methods to achieve superior responses from the experiments. The most usual methods are: X-ray and neutron diffraction - XRD, extensometric techniques such as blind hole, cut ring, cut by section removing layers. The XRD is considered a nondestructive method for superficial residual stress measurements. Applied stress, as an external load, is usually highest at the surface where the failures start over [10, 11].

It is proposed the analysis of the thermal cycle of welding and residual stress of the DSS welded plates for application in new container for radiopharmaceuticals transport. Temperature curves were acquired during welding in regions near the melting pool. These results must to be linked with residual stress data obtained after welding process in order to assure better safety during transport to the fabricated parts.

2. EXPERIMENTAL

The specimens produced in the dimensions of 72 x 72 x 1.8 mm^3 were welded (butt joint) autogenously by the GTAW process in the Welding Laboratory of the Federal University of Espírito Santo (LabSolda/DEM/UFES). Table 1 shows the chemical composition of UNS S32304 duplex stainless steel used in the experimental work. The alloy's chemical composition was certified by the commercial supplier Aperam Inox América do Sul S/A.

The pulsed current and direct polarities were used with automatic drive systems. The samples were fixed in order to reproduce the conventional welding process, as shown in Fig. 1. A batch of samples was welded with commercial argon protection gas and one with a mixture of argon and 2% of nitrogen. The gas flow rate in both cases was 10 $L.min^{-1}$.

Table 1: Chemical composition (% mass and ppm) of the duplex stainless steel UNS S32304.

Cr	Ni	Mo	Mn	Si	C	P	S	Ti	Cu	Co	N ppm
22.2	3.5	0.2	1.4	0.25	0.02	0.02	0.001	0.004	0.41	0.091	1030

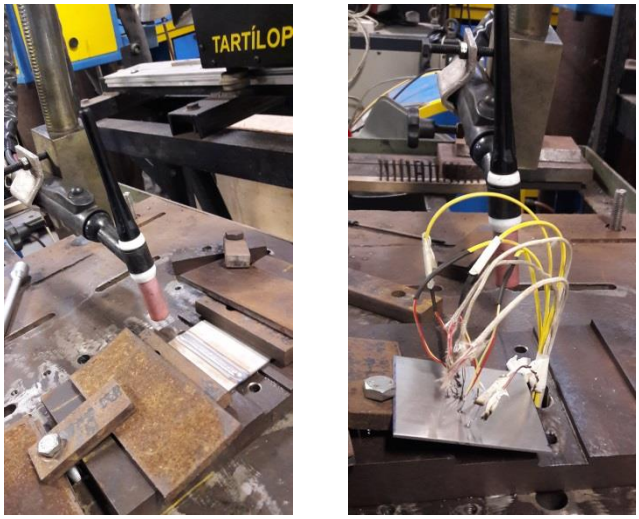

Figure 1: Welding arrangement for the duplex stainless steel UNS S32304 thin plates.

The American Welding Society - AWS Class EWTh-2 electrode was remained negative being located at 2 mm with a 90° angle from the plate, according to direct polarity process. The electrical current and voltage values were measured for each welding step. In the case of the pulsed current, the wave was maintained in balance with background time and pulse values equal to 0.9 s. In Table 2, it is shown the welding and thermal cycle parameter.

Regarding the parameters such as voltage (U), pulsed and background current (I_p, I_b), pulsed and background time (t_p, t_b), the welding speed (v) along with 0.6 arc efficiency for the pulsed GTA welding, it was possible to calculate the welding heat input (H) per mm using Eq. 1 [6]. The welding heat input shown in Table 2 was determined using the average voltage, current and the average weld speed.

$$H = \frac{60.U.(Ip.tp+Ib.tb)}{(tp+tb).v} \quad (1)$$

The temperature was measured and recorded using thermocouples type K attached to a data acquisition system. Four thermocouples were positioned and fixed to the sample plate's surface (Fig. 2) using high voltage capacitive discharge generator at different distances, along transversal and longitudinal lines of the weld bead. The thermocouples were located at 2.0 mm, 3.0 mm, 4.0 mm and 5.0 mm from the joint line.

Table 2: Welding parameters used for the pulsed GTAW process.

Sample	#WA	#WAN
Shielding gas *(10L.min^{-1})*	Pure Argon	Ar+2%N_2
Voltage	11 V	11 V
Pulse current (I_p)	150 A	140 A
Background current (I_b)	80 A	70 A
Pulse time (t_p)	0.9 ms	0.9 ms
Background time (t_b)	0.9 ms	0.9 ms
Welding speed	35 cm.min^{-1}	35 cm.min^{-1}
Arc efficiency	60%	60%
Heat Input	0.20 kJmm^{-1}	0.17 kJmm^{-1}

The signals from the thermocouples were acquired with an 8-channel universal data acquisition system (DAQ) amplifier using MX board - PT1000 for room temperature automatic conditioning. The measured total error limit at 300 K ambient temperature is ± 1 K and the temperature drift (type K) was used K/10K ratio where the uncertainty was ≤ ± 0.5.

The XRD used method was multiple exposure technique, according to SAE International, former Society of Automotive Engineers, SAE HS-784 standard [12], which it is possible to obtain more precise determination of ψ, where ψ is the angle between the normal (Ns) of the sample and the normal of the diffracting plane (bisecting the incident and diffracted beams), using more than two ψ orientations, and ψ plotting the measured strain values for each ψ orientation as function of sen^{2}ψ. Measurements were made transversal to the weld bead for the sample as received and also for surface profiles for location in solidified zone (SZ), heat-affected zone (HAZ) and base metal (BM). The distances for each measurement are shown in Table 3.

Table 3: All positions for residual stress measurement.

Phase	**Distance (mm)**									
	WZ	**HAZ**		**BM**						
Austenite	0.0	3.5	5.5	8.5	10	-	14	-	-	24
Ferrite	-	3.5	5.5	7.5	9.5	11.5	13.5	15.5	17.5	19.5

For the residual stress measurements in austenite phase, behavior of peak (420), an X-ray diffractometer was used in a Bragg-Brentano geometry and CuKα radiation (λ=0.154 nm). And then, to investigate the residual stress in ferrite phase, behavior of peak (211), an X-ray diffractometer was used in a pseudo-parallel geometry and CrKα radiation (λ=0.229 nm).

The sample was set at position ϕ=0° and, in some cases, ϕ=90° in the direction of rolling. The residual stresses were calculated by the sin^{2}ψ method. For the determination of position 2θ of the analyzed peak, the localization method was used according to intensity using the mathematical function Pearson7A [13] with the help of the graphical program Fityk [14]. The choice of function was based on the literature and on the correlations obtained when

comparing the results with other functions. For this analysis, the elastic constants are shown in Table 4.

Table 4: Elastic constants of the phases analyzed in the rolling direction [15].

Phase	Poisson coefficient (ν)	Modulus of elasticity (E) GPa
Austenite	0.305	190
Ferrite	0.186	201

3. RESULTS AND DISCUSSION

3.1 Thermal cycle

In Fig. 2, it is shown plates after the pulsed GTAW welding process along with the positions of the thermocouples. Note that for sample on the right side using Ar+2%N_2 it has a larger weld bead width and more damaged in weld zone than sample welded with pure argon as shielding gas.

The temperature distributions for the four thermocouples, it was plotted for both specimens as shown in Fig. 3. First, for Fig. 3 (a) the thermocouples TK1 and TK2 (2.0 mm distant from the melting pool) were placed closer to the weld bead where the temperatures were near to 711 °C and 622 °C, respectively. Through the TK3 and TK4 thermocouples it is shown the symmetric temperature peaks in regions close to the interface of the HAZ to the BM for sample welded pure argon as shielding gas.

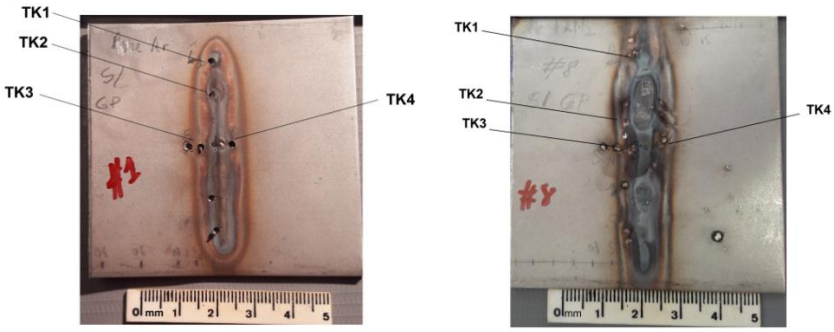

Figure 2: The welded plates with thermocouples location. In left hand, the weld plate #WA using pure Ar and the right hand the sample #WAN with Ar+2%N_2 as shielding gas.

In the thermal cycle for sample Ar+2%N_2 as shown in Fig. 3 (b), a temperature peak near 736 °C is observed for thermocouple TK1 (2.0 mm distant from the melting pool) being about 25 °C more than pure argon sample considering the same region. Y. C. Lin [16], also showed a peak temperature of a thermal cycle increased with increasing nitrogen content in the shielding gas. Thus, increasing the nitrogen content it is carried more heat into the workpiece and increases the weld metal area. In addition, according to the studies by K. H. Tseng and C. Chou [6], using pulsed GTAW process a greater amplitude ratio can reduce the temperature difference between the fusion zone and unaffected base metal in weldment and therefore the welding residual stress can be reduced.

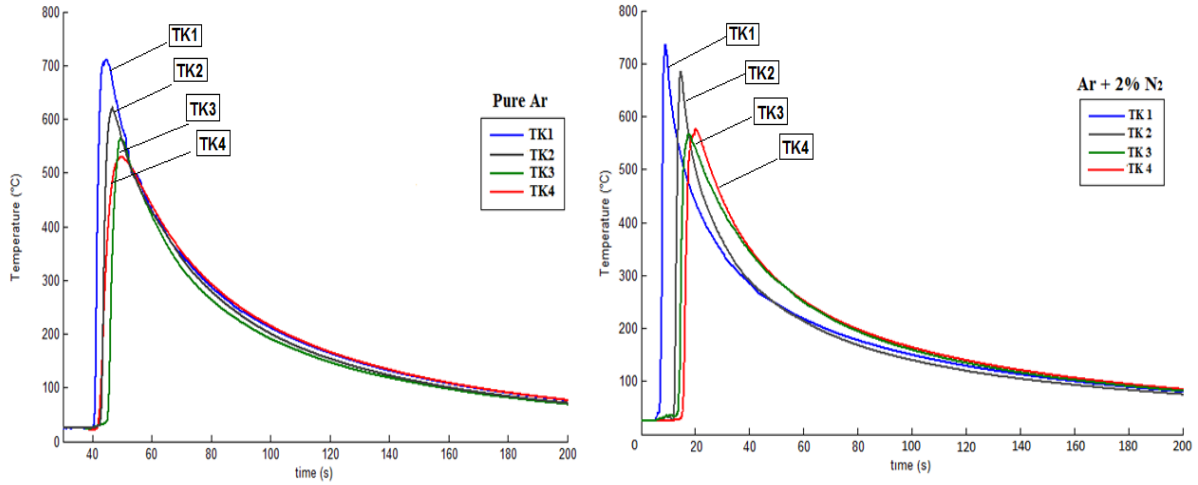

Figure 3: Distribution of temperatures for samples (a) Pure Ar and (b) Ar + 2%N_2 showing the temperature variation measured with each thermocouple for the UNS 32304 duplex stainless steel, 1.8 mm long stripe, while being welded.

3.2 Residual stress

In the Fig. 4 it is showed the graph of the microstrain ε x $\sin^2\psi$ for the material as received. It is observed that the slopes of the data are decreasing, indicating that the residual stresses have a compressive behavior, with values -263 ± 15 MPa for the austenite and around of -192 ± 17 MPa for the ferrite phase.

As seen in Fig. 5, a stress profile was found for the different phases of the samples. It is observed that in the sample welded only with pure argon, the solidified zone presented lower residual tensile strength, compared to the sample welded with shielding gas composed by the mixture argon and nitrogen. For both samples, there is a decrease in the stress value for both samples from the heat-affected zone until compressive residual stresses. It is also observed that the sample welded with argon and nitrogen has compressive values starting at 10 mm from the center of the solidified zone, whereas the sample welded with pure argon only from 14 mm (Fig. 5(a)). This is can be linked to the peak temperature using Ar + 2% N_2 as shielding gas observed in Fig. 4(b).

For regions close to the heat source, the results of residual stress obtained for the austenite, shows an increase of the stress in relation to the value found for the as received sample. This may be related to recrystallization/grain growth of the phase in this region [16].

According to Fig. 5, the addition of nitrogen leads to a slight increase in the residual stress of the phases. In the study made by Muthupandi et al. [17], the Ar-N_2 mixture has a higher ionization potential, increasing the welding energy and also the peak temperature. Lundin et al. [18] describe that additions of diatomic gases cause contraction in the contours of the plasma near the anode, in addition it is mentioned that the addition of nitrogen increases the efficiency of the arc reducing the losses of heat. For Lin et al. [19], it was observed that with the addition of nitrogen, the peak temperature increases and consequently the residual stresses of the austenitic steels too.

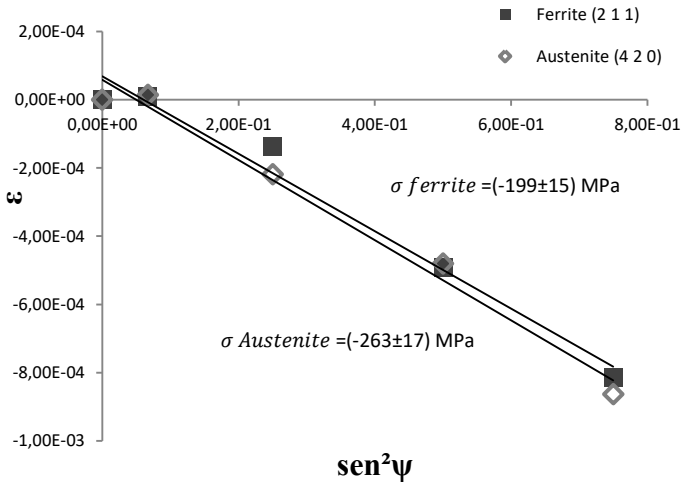

Figure 4: The graph of microstrain ε x sin²ψ for the material as received.

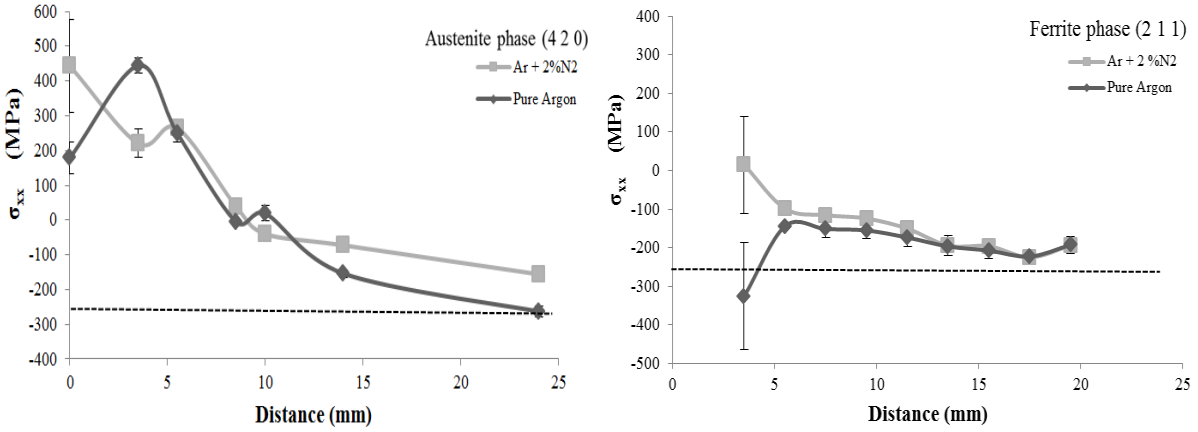

a) b)

Figure 5: Residual stress profiles of the austenite (a) and ferrite phases (b) of the duplex stainless steel UNS S32304 welds.

4. CONCLUSION

Based on the experimental results from type UNS S32304 after welding, the following conclusions are drawn.

The measurement of residual stresses in samples treated by X-ray diffraction using the $\sin^2 \psi$ method indicated that the effect of the welding thermal cycle on the heterogeneous microstructure causes the development to tensile residual stress in solidified zone and inverse (compressive) residual stress around 10-13 mm range from weld joint for both sample.

Comparison for both samples revealed that the stress state is more affected for mixture using Ar+2%N_2 as shielding gas. For this atmosphere, all peaks temperature which are slightly higher than the pure argon gas sample. Additional, welds subjected to ionizing radiation doses have a reduced capacity to resist corrosion and impact toughness, being especially true for welds made without an appropriated atmosphere. Finally, it is suggested to take further

investigation about gamma radiation interaction in weld samples for application in safe equipment's as Type B packages.

ACKNOWLEDGMENTS

The authors would like to express their gratitude to the colleagues of the Federal University of Espírito Santo (UFES) responsible of the Welding Laboratory (LabSolda) for the cooperation during welding preparation. Special thanks to CAPES and CNPq Brazil for financial support.

REFERENCES

1. D. H. S. Hara, M. Fiore, R. F. Lucchesi, V. A. Mancini, J. L. Rossi, "Materials selection for a transport packaging of Mo-99", *International Nuclear Atlantic Conference* - INAC, 2015, São Paulo-SP, Brazil, 4-9 Oct., pp. 1-7 (2015).
2. F. C. Cione, M. A. Rizzutto, F. F. Sene, A. C. Souza, E. G. Betini, J. L. Rossi, "The shielding against radiation produced by powder metallurgy with tungsten copper alloy applied on transport equipment for radio-pharmaceutical products", *International Nuclear Atlantic Conference* - INAC, 2015, São Paulo-SP, Brazil, 4-9 Oct., pp. 1-9 (2015).
3. T. Kannan, N. Murugan, "Effect of flux cored arc welding process parameters on duplex stainless steel clad quality", *Journal of Materials Processing Technology*, Vol. 176.1**,** pp. 230-239, (2006).
4. E. G. Betini, F. C. Ceoni, C. S. Mucsi, R. Politano, M. T. D. Orlando, J. L. Rossi, "Study of the temperature distribution on welded thin plates of duplex steel to be used for the external clad of a cask for transportation of radiopharmaceuticals products", *International Nuclear Atlantic Conference* - INAC, 2015, São Paulo-SP, Brazil, 4-9 Oct., pp. 1-6 (2015).
5. "Radioactive Materials Transportation". *Standard CNEN NE 5.01* Resolution CNEN 013/88Aug.1988.Available in http://appasp.cnen.gov.br/seguranca/normas/pdf/Nrm501.pdf (2017). Assessed in 2 Jun., 2017. (In Portuguese)
6. Y. Jiang, H. Tan, Z. Wang, J. Hong, L. Jiang, J. Li, "Influence of Cr_{eq}/Ni_{eq} on pitting corrosion resistance and mechanical properties of UNS S32304 duplex stainless steel welded joints", *Corrosion Science*, Vol. 70, pp. 252-259, (2013).
7. K. H. Tseng and C. Chou, "The effect of pulsed GTA welding on the residual stress of a stainless steel weldment", *Journal of Materials Processing Technology,* Vol. 123.3, pp. 346-353, (2002).
8. V. I. Monin, R. T. Lopes, S. N. Turibus, J. C. Payão Filho, J. T. D. Assis, "X-Ray diffraction technique applied to study of residual stresses after welding of duplex stainless steel plates", *Materials Research*, Vol. 17, pp. 64-69 (2014).
9. C. S. C. Machado, M. X. Milagre, M. T. D. Orlando, J. L. Rossi, T. S. Luz, M. C. S. Macêdo, J. N. Chagas, "Effect of protection gas in the residual stress profile of UNS S32304 stainless steel welded with TIG", *Blucher Proceedings - IV Workshop of Applied Crystallography to Materials Science and Engineering*, Vitória - ES, Brazil, 23-25 May, Vol. 2, pp.1-4 (2014). (In Portuguese).
10. F. J. Cárcel-Carrasco, M. Pascual-Guillamón, M. A. Pérez-Puig, "Effects of X-rays radiation on AISI 304 stainless steel welding with AISI 316L filler material: A study of resistance and pitting corrosion behavior", *Metals*, Vol. 6.5, pp. 102 (2016).

11. B. D. Cullity, *Elements of X-Ray Diffraction*. Second Edition, Addison Wesley Inc., New York & USA (2001).
12. F. C. Cione, A. C. Souza, L. G. Martinez, J. L. Rossi, E. G. Betini, F. Rola, M. A. Colosio, "Measurements of residual stresses in aluminum wheels using the techniques of XRD, strain gages and FEA simulation - a comparison", *SAE International Journal Materials and Manufacturing*, Vol. 9, pp. 1-3 (2016).
13. SAE International. *Residual Stress Measurement by X-ray diffraction*, HS-784, Edition. ISBN 0-7680-1069, (2003).
14. P. J. Withers, H. K. D. H. Bhadeshia, "Residual stress. Part 1 – Measurement techniques", *Materials Science and Technology*, Vol. 17, pp. 355-365 (2001).
15. M. Wojdyr, "Fityk: a general-purpose peak fitting program", *Journal of Applied Crystallography*, Vol. 43, pp. 1126-1128 (2010).
16. J. Johansson, M. Odén, X. H. Zeng, "Evolution of the residual stress state in a duplex stainless steel during loading", *Acta Metallurgica*, Vol. 47.9, pp. 2669-2684 (1999).
17. Y. Lin and P. Chen, "Effect of nitrogen content and retained ferrite on the residual stress in austenitic stainless steel weldments", *Materials Science and Engineering A*, Vol. 307, pp. 165-171 (2001).
18. C. C. Hsieh, D. Y. Lin, M. C. Chen, W. Wu, "Precipitation and strengthening behavior of massive d-ferrite in dissimilar stainless steels during massive phase transformation", *Materials Science and Engineering A*, Vol. 477, pp. 328-333 (2008).
19. V. Muthupandi, P. B. Srinivasan, S. K. Seshadri, S. Sundaresan, "Effect of nitrogen addition on formation of secondary austenite in duplex stainless steel weld metals and resultant properties", *Science and Technology of Welding and Joining*, Vol. 9, pp. 47-52 (2004).